*Pharmaceutical Research, Vol. 25, No. 6, June 2008 (© 2008)*
DOI: 10.1007/s11095-008-9543-1

*Research Paper*

# Targeted Intestinal Delivery of Supersaturated Itraconazole for Improved Oral Absorption

**Dave A. Miller,[1] James C. DiNunzio,[1] Wei Yang,[1] James W. McGinity,[1] and Robert O. Williams III[1,2]**

*Received November 7, 2007; accepted January 22, 2008; published online February 21, 2008*

***Purpose.*** To investigate the use of Carbopol® 974P as a stabilizing agent for supersaturated levels of itraconazole (ITZ) in neutral pH aqueous media and the resultant effects on oral absorption of ITZ.
***Methods.*** Carbopol® 974P was incorporated into an EUDRAGIT® L 100-55 carrier matrix at concentrations of 20% and 40% based on polymer weight with the aim of prolonging supersaturated ITZ release from the enteric matrix. Amorphous solid dispersions of ITZ in EUDRAGIT® L 100-55 containing either 20% or 40% Carbopol® 974P were produced by hot-melt extrusion (HME). Solid state analysis of these compositions was performed using differential scanning calorimetry and qualitative energy dispersive X-ray spectroscopy. Dissolution analysis was conducted using a pH change method. Oral absorption of ITZ was evaluated in male Sprague–Dawley rats.
***Results.*** Solid state analysis demonstrated that the extruded compositions were entirely amorphous and homogenous with respect to drug distribution in the polymer matrix. Dissolution analysis revealed that the addition of Carbopol® 974P to the EUDRAGIT® L 100-55 carrier system functioned to prolong the release of supersaturated levels of ITZ from the EUDRAGIT® L 100-55 matrix following an acidic-to-neutral pH transition. In vivo evaluation of ITZ absorption revealed that the addition of Carbopol® 974P substantially reduced the absorption variability seen with the EUDRAGIT® L 100-55 carrier system. In addition, the 20% Carbopol® 974P formulation exhibited a five-fold improvement in absorption over our initially reported ITZ particulate dispersion compositions that limited supersaturation of ITZ primarily to the stomach.
***Conclusions.*** The results of this study strongly suggest that substantial improvements in oral antifungal therapy with ITZ can be achieved via intestinal targeting and polymeric stabilization of supersaturation.

**KEY WORDS:** hot-melt extrusion; intestinal targeting; itraconazole; oral absorption; supersaturation.

## INTRODUCTION

In a previous report (1), we proposed that the primary site of itraconazole (ITZ) absorption from the gastrointestinal (GI) tract is the proximal small intestine. In a subsequent report (2), this hypothesis was confirmed by the substantial improvement in ITZ absorption that resulted from solid dispersion systems that either generate or maintain supersaturated concentrations of ITZ in neutral pH media following the transition from an acidic environment. By these two studies, we demonstrated that supersaturated concentrations of ITZ must be targeted to the small intestine since adequate absorption is not attained when supersaturation is primarily limited to the gastric environment.

ITZ is optimally absorbed in the small intestine because of the vastly greater mucosal surface area through which drug permeation can occur *versus* the stomach. Snyder *et al.* reported the absolute surface area of the human stomach and small intestine to be 0.053 and 200 $m^2$, respectively (3). The relatively smooth surface of the gastric mucosa *versus* the convoluted intestinal mucosa consisting of plicae circulares, villi, and microvilli account for the approximate 4,000-fold increase in mucosal surface area between these two regions of the GI tract (4,5). Moreover, the lamina propria of the small intestine is richly vascularized and therefore aptly suited for transfer of molecules from the intestinal lumen into systemic circulation (4). When considering the anatomy of the upper GI tract it becomes apparent that limiting ITZ dissolution to the gastric environment would produce only minimal absorption, and conversely absorption of ITZ in the small intestine will be directly proportional to dissolution. As supersaturation is typically a transient event, particularly for ITZ in neutral media, it can be understood that delaying the onset of supersaturation until the drug enters the primary site for absorption would maximize the exposure of the intestinal mucosa to dissolved ITZ.

Although numerous prior articles have demonstrated improved oral bioavailability of poorly water-soluble drugs via supersaturatable formulations (6–10), few studies have been published that illustrate specific targeting of drug supersaturation to the intestinal lumen by the use of pH-dependant carrier polymers. In one such study, Kondo *et al.* evaluated co-precipitate solid dispersion systems with pH-independent polymeric carriers (povidone (PVP) and copolyvidone) as well as a pH-dependant polymeric carrier [hypromellose phthalate

[1] College of Pharmacy, University of Texas at Austin, Austin, Texas 78712, USA.
[2] To whom correspondence should be addressed. (e-mail: williro@mail.utexas.edu)

(HP-55)] as a means of improving the bioavailability of the anticancer drug HO-221 (11). *In vivo* studies conducted with these formulations revealed that absorption of HO-221 achieved with the HP-55 formulation was twice that of the PVP and copolyvidone co-precipitates. This outcome was hypothesized to be the result of targeting the onset HO-221 supersaturation to the small intestine *versus* the stomach. It was speculated that transient supersaturation resulted in poor absorption with the pH-independent formulations due to precipitation of HO-221 before passage into the small intestine. Conversely, the pH-dependant HP-55 carrier confined supersaturation of HO-221 to the small intestine and maximized the exposure of absorptive surface area to elevated drug concentrations. This hypothesis was confirmed after intraduodenal administration of the copolyvidone formulation produced plasma concentrations which slightly exceeded that of the HP-55 co-precipitate formulation.

Kohri *et al.* also evaluated a pH-dependant solid dispersion system to improve the absorption of albendazole, a poorly water-soluble drug with a pH solubility profile similar to ITZ (12). The intestinal absorption of albendazole was found to be variable and highly dependant on gastric pH (13). These researchers thus evaluated the use solid dispersion systems with HP-55 to improve the intestinal absorption of albendazole. *In vitro* dissolution testing confirmed that HP-55 improved albendazole supersaturation following pH shift from 1.2 to 6.5. *In vivo* studies were conducted with an HP-55/hypromellose combination formulation which generated a 3.2-fold improvement in bioavailability compared to crystalline drug in rabbits with elevated gastric pH. This improvement was attributed to the targeted supersaturation of albendazole to the small intestine resulting from the pH-dependant drug release of the solid dispersion formulation.

In our previous report (2), it was demonstrated that the polymeric carriers Methocel™ E50 and EUDRAGIT® L 100-55 for amorphous ITZ solid dispersions produced substantially greater *in vivo* absorption than our previously presented immediate release formulations (1) owing to improved supersaturation of ITZ in the small intestine. Methocel™ E50 was identified as the preferred formulation due to reduced variability over the EUDRAGIT® L 100-55 formulation; however, the EUDRAGIT® L 100-55 formulation exhibited the potential for prolonging ITZ absorption presumably by extending the release of ITZ from the polymeric matrix along the small intestine. The variability of the EUDRAGIT® L 100-55 based formulation was attributed to poor stabilization of ITZ supersaturation at neutral pH by the polymer which was demonstrated *in vitro* by pH change dissolution testing. It was hypothesized that the addition of a polymeric additive to the EUDRAGIT® L 100-55 carrier that would act to improve the stability of supersaturated ITZ in neutral media would provide more consistent supersaturation along the small intestine and ultimately improve absorption while reducing variability.

It was discovered in our previous paper (2) that the optimal polymeric stabilizers of supersaturated ITZ solutions are high molecular weight polymers with abundant acidic functional groups. Strong intermolecular interactions (likely hydrogen bonding) in solution coupled with high local viscosity were identified as the underlying causes for the stabilization that resulted from these polymer attributes. Therefore, these characteristics were foremost considered when identifying possible stabilizing polymeric additives for incorporation into EUDRAGIT® L 100-55-solid dispersion formulations.

The Carbopol® family of polymers consists of high molecular weight polyacrylic acids crosslinked to varying degrees with either allyl sucrose or allyl ethers of pentaerythritol. Carbopol® polymers contain between 56% and 68% carboxylic acid groups based on dry polymer mass (14). The viscosity of Carbopol® dispersions (0.5 wt%) at neutral pH ranges from 4,000 to 60,000 mPa·s (14). Owing to the number of acidic functional groups on the polymer and immense solution viscosities at neutral pH, Carbopol® polymers were identified as potentially ideal stabilizers for supersaturated ITZ solutions. In this study, Carbopol® 974P was selected for investigation as a polymeric stabilizer of supersaturated ITZ because of its intermediate viscosity on the spectrum of Carbopol® polymer grades. This intermediate viscosity was expected to allow for substantial stabilization of ITZ in solution without severely retarding drug release.

Specifically, the aim of this study was to evaluate the incorporation of Carbopol® 974P into an EUDRAGIT® L 100-55-based solid dispersion system with regard to stabilization of ITZ supersaturation and enhancement of oral absorption. The initial objective of the study was to determine the morphology and dispersed state of ITZ following HME processing with carrier systems consisting of EUDRAGIT® L 100-55 with 20% and 40% (*w*/*w*) Carbopol® 974P additive. The second objective was to investigate the *in vitro* dissolution properties of the Carbopol® 974P-containing formulations in comparison to the EUDRAGIT® L 100-55 carrier system by a pH change dissolution test methodology. The final objective of this study was to investigate the effect of the Carbopol® 974P additive at levels of 20% and 40% on the *in vivo* absorption of ITZ from the EUDRAGIT® L 100-55-based amorphous solid dispersion systems.

## MATERIALS

Itraconazole, BP micronized was purchased from Hawkins, Inc. (Minneapolis, MN). EUDRAGIT® L 100-55 was purchased from Degussa GmbH (Linden, NJ). Carbopol® 974P was provided by Lubrizol Advanced Materials Inc. (Cleveland, OH). Triethyl citrate (TEC, NF) was provided by Vertellus™ Performance Materials, Inc. (Greensboro, NC). HPLC grade Acetonitrile was purchased from EMD chemicals (Darmstadt, Germany). All other chemicals used in this study were of ACS grade.

## METHODS

### Hot-Melt Extrusion (HME)

All hot-melt extruded compositions presented in this study were produced with a HAAKE Minilab II Micro Compounder (Thermo Electron Corporation, Newington, NH) equipped with twin, co-rotating conical screws (5/14 mm diameter). All formulation components were premixed in a glass mortar and pestle prior to extrusion. The blending of the plasticizer with the polymers was conducted prior to the blending of ITZ with the polymer carrier system. The ITZ content for all composi-

**Table I.** Formulation Summary for HME Processed ITZ/EUDRAGIT® L 100-55 Amorphous Solid Dispersions with Carbopol® 974P Additives

| Formulation Name | Formulation Components (Parts) | | | |
|---|---|---|---|---|
| | ITZ | EUDRAGIT® L 100-55 | Carbopol® 974P | TEC |
| 20% Carbopol® 974P[a] | 3 | 4 | 1 | 1 |
| 40% Carbopol® 974P[a] | 3 | 3 | 2 | 1 |
| EUDRAGIT® L 100-55 | 3 | 5 | 0 | 1 |

[a] Based on polymer weight in carrier formulation

tions was 33% (*w*/*w*) and only the ratio of EUDRAGIT® L 100-55 to Carbopol® 974P was modulated. A summary of the formulations presented in this study is provided in Table I. Powder blends were fed into the extruder barrel via the Minilab manual force-feeding device. No external die was applied at the outlet of the extruder barrel, and therefore extruded materials were forced through the 1.0×4.0 mm rectangular outlet port. All formulations presented in this study were extruded at a processing temperature of 130°C and a screw speed of 300 rpm. Motor torque for all formulations was in the range of 200–250 N·m. After HME processing, extrudates were ground in a blade grinder (Capresso Inc., Closter, NJ) for 2 min. The ground product was then passed over a 60 mesh sieve. The material which passed through the sieve was manually milled in a porcelain mortar and pestle for 1 min to yield a fine powder. All further analysis was then conducted on this finely milled powder.

### Differential Scanning Calorimetry (DSC)

Modulated DSC analysis was conducted using a TA Instruments Model 2920 DSC (New Castle, DE) equipped with a refrigerated cooling system. Samples were weighed to 15±5 mg in aluminum crimped pans (Kit 0219-0041, Perkin-Elmer Instruments, Norwalk, CT). Samples were heated at a ramp rate of 10°C/min from 5 to 215°C with a modulation temperature amplitude of 0.5°C and a modulation period of 40 s for all studies. Ultrahigh purity nitrogen was used as the purge gas at a flow rate of 40 ml/min. All data analyses were performed using TA Universal Analysis 2000 software. The thermogram for amorphous ITZ used in the DSC analysis of the solid dispersions formulations was obtained on a second heating of crystalline ITZ following an initial heating to 215°C followed by rapid cooling (20°C/min) to 5°C. The $T_g$s of the EUDRAGIT® L 100-55 and Carbopol® 974P polymers were determined by first run DSC following preheating of the polymer powders to 90°C for 15 min in an MF-50 model moisture analyzer (AND Company Ltd. Encino, CA) to expel absorbed moisture. Cell constant and temperature calibrations were conducted with the use of an indium standard prior to instrument operation. The results of DSC analysis were evaluated in terms of both forward and reverse components of heat flow. All notable thermal events were captured and more clearly illustrated by the reversing component of heat flow, and therefore all DSC results presented herein are in terms of reverse heat flow.

### Energy Dispersing X-ray Spectroscopy (EDS)

Samples were prepared by dispersing ground extrudate powder onto a 200 mesh copper grid coated with a carbon support film (Electron Microscopy Sciences, Hatfield, PA). Imaging and energy dispersing X-ray spectroscopy (EDS) were conducted using a JEOL 2010F transmission electron microscope (JEOL USA, Inc., Peabody, MA) equipped with a HAADF scanning transmission electron microscope (STEM) detector, Oxford spectrometer and GATAN digital imaging system operated at 200 kV.

### Dissolution Testing

Dissolution testing was performed according to USP 29 Apparatus 2 guidelines (paddle method) at 50 rpm in a Vankel 7000 Dissolution Tester (Vankel Technology Group, Cary, NC) equipped with a VK 8000 model autosampler. The dissolution method utilized was in accordance with the USP 29 dissolution testing specifications for delayed-release dosage forms Method A. Specifically, formulations were first subjected to "acid stage" testing (2 h in 750 ml of 0.1 N HCl) followed by a pH adjustment to 6.8±0.5 by the addition of 250 ml of 0.2 M tribasic sodium phosphate to start the "buffer stage" testing which was conducted for four additional hours. The 250 ml of 0.2 M tribasic sodium phosphate was added to the 750 ml of 0.1 N HCl rapidly from a beaker to avoid hot-spot formation during the pH adjustment phase (15). The dissolution media was held at 37.0±0.2°C throughout the test procedure. No surfactant was included in the media during either phase of dissolution testing. To each dissolution vessel, 180 mg of the milled extrudate powder was added (60 mg ITZ equivalent). This amount of drug corresponded to a theoretical 80 μg/ml ITZ concentration for the acid phase of testing which represents a 20-fold level of supersaturation assuming an equilibrium solubility of 4 μg/ml in 0.1 N HCl (16). All aliquots of dissolution media were filtered using one 0.45 μm and one 0.2 μm nylon membrane syringe filter in series (Whatman®, Florham Park, NJ). Filtered aliquots were then diluted in a 1:1 ratio with HPLC mobile phase.

Dissolution samples were analyzed for drug content using a Waters (Milford, MA) high performance liquid chromatography (HPLC) system with a photodiode array detector (Model 996), and extracting at a wavelength of 263 nm. An auto sampler (Model 717 Plus) was used to inject 200 μl samples, and the data were collected and integrated using Empower® Version 5.0 software. The column used was a Phenomenex® Luna 5 μm C18(2) 100 A, 150×4.6 mm (Phenomenex®, Torrance, CA). The mobile phase consisted of 7:3 (*v*/*v*) acetonitrile/deionized water with 0.5 ml/l of diethanolamine. The retention time of itraconazole was approximately 6 min. Linearity was demonstrated from 0.024 to 100 μg/ml ($r^2 \geq 0.999$) and the relative standard deviation of three injections was less than 0.5%.

### *In vivo* Studies

Institutionally approved *in vivo* studies were conducted using CD® IGS Sprague–Dawley rats (Charles River Laboratories, Inc., Wilmington, MA), which were pre-catheterized with a vascular catheter surgically inserted into the jugular vein. All rats were received between 275 and 325 g total body weight. The catheter was flushed daily with 0.3 ml of 50 U/ml heparinized normal saline. After at least 3 days of acclimatization period, the rats were administered the aqueous dispersion of the formulations by oral gavage at a dose of 30 mg ITZ/kg body weight ($n$=4). Each formulation was dispersed in deionized water just prior to dosing such that 400 μl of suspension contained a dose of 9 mg ITZ. Serial blood samples (approximately 0.3 ml each) were withdrawn through the jugular vein catheter at 0, 2, 3, 3.5, 4, 4.5, 5, 5.5, 6, 8, 12 and 24 h after dosing and placed into a pre-heparinized microcentrifuge tube. Equal volumes of saline were replaced after each sampling. Plasma samples were harvested by centrifugation of the blood at 3,000×$g$ for 15 min and were kept at −20°C until drug analysis.

### Plasma Extraction and Chromatographic Analysis

Calibration standards and plasma samples were analyzed according to previously published methods (17,18). Briefly, upon thawing a volume of harvested plasma was transferred to a clean 1.5 ml microcentrifuge tube. Barium hydroxide 0.3 N (50 μl) and 0.4 N zinc sulfate heptahydrate solution (50 μl) were then added followed by vortex mixing for 30 s to precipitate water-soluble proteins. Acetonitrile (1 ml) containing 1,200 ng/ml ketoconazole as an internal standard was added to each plasma sample followed by vortex mixing for 1.5 min. The samples were then centrifuged at 3,000×$g$ for 15 min. The supernatants were then extracted and transferred to a clean 1.5 ml centrifuge tube and seated in an aluminum heating block (70°C), under a stream of nitrogen until dry. Samples were reconstituted with 250 μl mobile phase (62% acetonitrile/38% 0.05 M potassium phosphate monobasic buffer adjusted to pH 6.7 with NaOH) and vortex mixed for 1 min. The samples were then centrifuged for an additional 15 min and subsequently a 150 μl aliquot of the supernatant was extracted and filled into low volume HPLC vial inserts. Each sample was analyzed using the previously described Waters HPLC system. A Phenomenex® Luna 5 μm C-18(2) 100 A HPLC column (250×4.6 mm) was used in the analysis. The column was maintained at a temperature of 37°C for the duration of the injection set. The ITZ peak eluted at 14.6 min and the ketoconazole peak eluted at 5.3 min at a flow rate of 1.0 ml/min. The injection volume was 100 μl, and the wavelength of absorption was 263 nm. The limit of detection and quantitation for ITZ was 10 and 30 ng/ml, respectively.

### Pharmacokinetic Analysis

Non-compartmental analysis for extravascular input was performed on the data using WinNonlin version 4.1 (Pharsight Corporation, Mountain View, CA). By this method of analysis $T_{max}$ and $C_{max}$ were determined directly from the empirical data, AUC was calculated by the linear trapezoidal method, and $t_{1/2}$ was determined by calculation of the lambda $z$ parameter. Statistical comparisons were performed by two-tailed Student's $t$ test assuming equal variances ($\alpha$=0.05).

## RESULTS AND DISCUSSION

### DSC Analysis of HME Processed Formulations

In our previous paper, we reported the production of an ITZ/EUDRAGIT® L 100-55 (1:2 $w/w$) solid solution when processed by HME at 130°C utilizing 20% TEC (based on polymer weight) as a plasticizer (2). The formation of this solid solution at a processing temperature approximately 40°C below the melt temperature of ITZ represents solubilization of ITZ by the molten polymer during processing and indicates excellent miscibility of ITZ with EUDRAGIT® L 100-55. Miscibility of ITZ with EUDRAGIT® L 100-55 was reported by Overhoff *et al.* at levels greater than 60% ($w/w$) drug loading (19). Qualitative evaluation of ITZ solubility in TEC revealed little to no solubility of ITZ in TEC, and considering the 3:1 ratio of ITZ to TEC in the formulation, it is likely that TEC only facilitates the solubilization of ITZ by increasing the plasticity of EUDRAGIT® L 100-55 at the processing temperature.

In contrast, Six *et al.* reported limited miscibility (13% $w/w$) of ITZ with EUDRAGIT® E 100 following HME processing at temperatures above the melting point of ITZ (20–22). When comparing the structures of EUDRAGIT® L 100-55 and EUDRAGIT® E 100, it becomes evident that the primary molecular attribute affecting the miscibility of ITZ with these polymers is the acidic functional groups contained on EUDRAGIT® L 100-55 that are not present on EUDRAGIT® E 100. Therefore, it appears that the acidic functional groups which were determined in our previous study (2) to improve the solubility of ITZ in aqueous media also enhance the miscibility of ITZ with acrylic polymers in the solid state. The affinity of weakly basic drugs with polymers containing acidic functional groups and the stabilizing effects of these polymers on such drug molecules in both the supersaturated solution state and amorphous solid state have been previously reported by Van Den Mooter *et al.* (23). These authors attributed the improved solution and amorphous state stability to the formation of a salt between basic drugs and acidic polymers. Owing to the abundance of carboxylic acid functional groups contained on the Carbopol 974P polymer network, it was expected that its incorporation into the EUDRAGIT® L 100-55 carrier matrix would not negatively impact the formation of an ITZ solid solution during HME processing.

The influence of the Carbopol® 974P additive on the ITZ/EUDRAGIT® L 100-55 HME processed formulations was evaluated at levels of 20% and 40% by polymer weight in the carrier system; i.e. EUDRAGIT® L 100-55 to Carbopol® 974P ratios of 4:1 and 3:2. To enable HME processing of these polymers at 130°C (below the onset of thermal degradation), 20% TEC (based on polymer weight) was incorporated into the carrier system. The ITZ loading in each formulation was 33%. A summary of these formulations is provided in Table I.

The DSC analysis of the 20% Carbopol® 974P formulation is presented in Fig. 1. The thermogram of the active HME processed formulation shows two glass transition temperatures ($T_g$) at 43°C and 134°C. The placebo extrudate

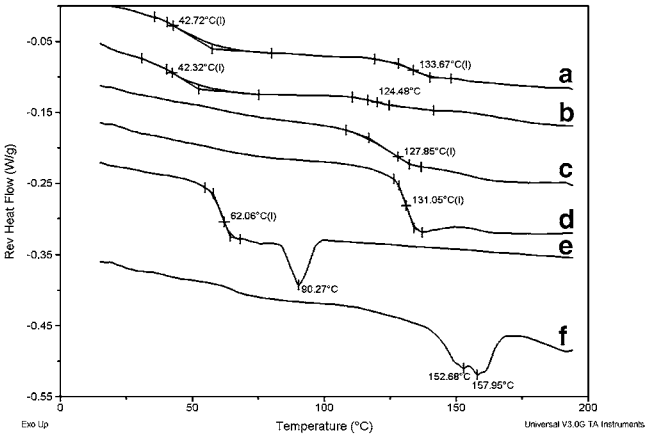


**Fig. 1.** DSC analysis of: (*a*) HME processed ITZ-containing 20% Carbopol® 974P additive formulation, (*b*) HME processed placebo 20% Carbopol® 974P additive formulation, (*c*) EUDRAGIT® L 100-55 powder, (*d*) Carbopol® 974P powder, (*e*) amorphous ITZ, (*f*) physical mixture of the active 20% Carbopol® 974P additive formulation.

also shows two similar $T_g$s at 42°C and 124°C; however, the second $T_g$ is shifted 10° downward and is less pronounced than that of the active extrudate. The $T_g$s of the EUDRAGIT® L 100-55 and Carbopol® 974P polymers were found to be 128°C and 131°C, respectively. Amorphous ITZ exhibits a $T_g$ at 62°C followed by two endothermic transitions at 75°C (not readily apparent on the displayed scale) and 90°C associated with the transition of a monotropic mesophase (24). Two melting endotherms are seen with the physical mixture at 153°C and 158°C both occurring below the melting point of ITZ (~170°C).

The two $T_g$s observed with the active and placebo HME processed formulations indicate immiscibility of EUDRAGIT® L 100-55 and Carbopol® 974P. This is attributed to the crosslinking of Carbopol® 974P which restricts the mobility of the polymer in the molten state, thereby limiting polymer chain intermingling. In our previous paper (2), the $T_g$ of EUDRAGIT® L 100-55 HME processed with 20% TEC was found to be 55°C, therefore the $T_g$s seen in Fig. 1 for both the active and placebo extrudates near 43°C indicates greater plasticization of the polymer. This is explained as a greater affinity of TEC for EUDRAGIT® L 100-55 than Carbopol® 974P. The $T_g$ reduction of Carbopol® 974P seen between the powder and the plasticized placebo extrudate (131°C to 124°C) supports this explanation as the plasticizer only slightly reduced the polymer $T_g$ indicating minimal Carbopol®-TEC interaction. Interestingly, ITZ appears to promote the immiscibility of Carbopol® 974P with both EUDRAGIT® L 100-55 and TEC. This is indicated by the upward shift in the $T_g$ of the Carbopol® 974P phase seen between the placebo and the active extrudates (124°C to 134°C). This may indicate a strong affinity of ITZ for Carbopol® 974P that disrupts the polymer's interactions with the other formulation components in the molten state during HME processing. The thermogram for the physical mixture seems to support this explanation as two endothermic events of similar magnitude occur approximately 5° apart. This reveals that roughly similar portions of crystalline ITZ are becoming solubilized independently into the separate EUDRAGIT® L 100-55 and Carbopol® 974P polymer phases. As considerably more EUDRAGIT® L 100-55 is contained in the formulation than Carbopol® 974P (4:1), the similarity in the solubilization of ITZ by the two polymer phases indicates that ITZ is preferentially solubilized by Carbopol® 974P over EUDRAGIT® L 100-55. The abundance of hydrogen bond donor sites on the Carbopol® 974P polymer may explain this result as more opportunities for intermolecular interactions with ITZ exist than with EUDRAGIT® L 100-55 in the molten state.

DSC analysis for the formulation containing 40% Carbopol® 974P revealed a similar result as seen in Fig. 2. Again, two $T_g$s are observed with both the active and placebo extrudates. The active formulation exhibits $T_g$s at 42°C and 133°C, while the placebo formulation shows $T_g$s at 42°C and 120°C. Compared to the 20% Carbopol® 974P formulation, the high temperature $T_g$ is more pronounced for both the active and placebo extrudates. This strongly suggests immiscibility of EUDRAGIT® L 100-55 and Carbopol® 974P as it appears that the magnitude of phase separation is dependant on the concentration of Carbopol® 974P in the formulation. The physical mixture for the 40% Carbopol® 974P formulation shows a large endotherm at 153°C and a smaller endotherm at 166°C indicating two populations of melting ITZ crystals. Compared to the physical mixture for the 20% Carbopol® 974P formulation, it appears that increasing the concentration of Carbopol® 974P in the formulation resulted in some consolidation of the two melting endotherms. The growth of the endotherm at 153°C that occurred by doubling the Carbopol® 974P concentration seems to substantiate the conclusion that ITZ has a stronger affinity for Carbopol® 974P than EUDRAGIT® L 100-55. With the previous formulation, at only 20% of the polymer system, Carbopol® 974P likely became saturated with ITZ and the overflow was then solubilized by molten EUDRAGIT® L 100-55. At 40% of the polymer carrier, Carbopol® 974 could solubilize a greater amount of ITZ, hence the growth of the endotherm at 153°C. The shift in size and position of the second endotherm

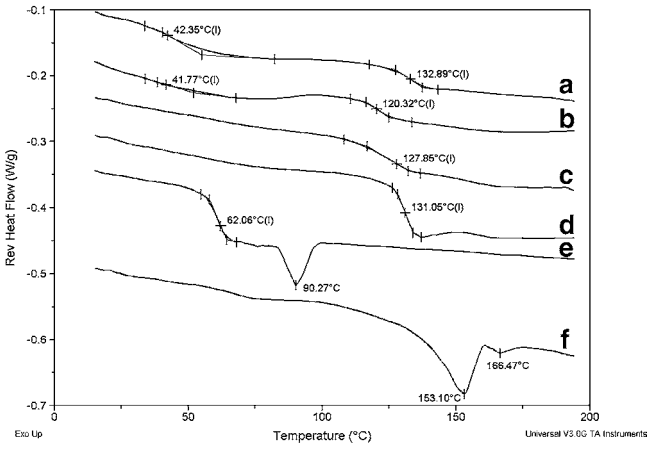


**Fig. 2.** DSC analysis of: (*a*) HME processed ITZ-containing 40% Carbopol® 974P additive formulation, (*b*) HME processed placebo 40% Carbopol® 974P additive formulation, (*c*) EUDRAGIT® L 100-55 powder, (*d*) Carbopol® 974P powder, (*e*) amorphous ITZ, (*f*) physical mixture of the active 20% Carbopol® 974P additive formulation.

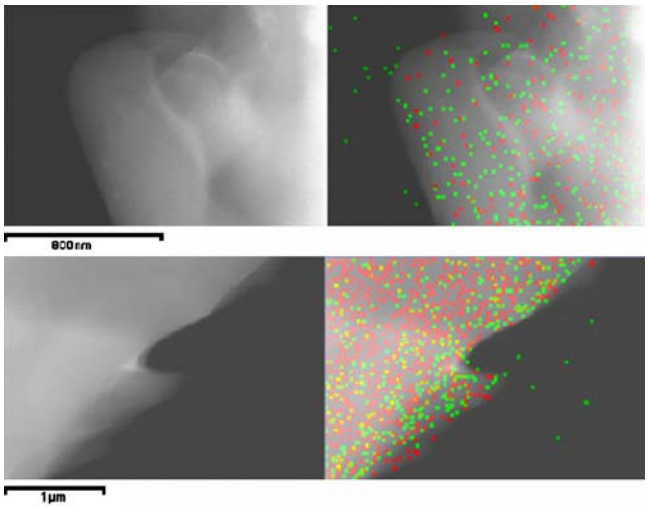


**Fig. 3.** EDS Mapping of ITZ/EUDRAGIT® L 100-55 (1:2; *top*) and 40% Carbopol® 974P additive (*bottom*) formulations. *Red* Cl, *green* N, *yellow* overlap of Cl and N. Note that nitrogen counts shown in EDS images outside of the sample are due to small amounts of nitrogen adsorbed on the copper film.

indicates that a small fraction of crystalline ITZ required more heat input to initiate melting. This could be due to crystalline ITZ in a saturated Carbopol® 974P phase that required more energy input to become solubilized by the polymer.

These DSC results suggest possible heterogeneity of the HME processed formulations with respect to drug distribution in the two polymer phases owing to a seemingly stronger affinity of ITZ for Carbopol® 974P over EUDRAGIT® L 100-55 in the molten state. However, it was seen in our previous report (2) that ITZ is readily solubilized by molten EUDRAGIT® L 100-55 during HME processing at 130°C and 300 rpm. Therefore, it was expected that the intense agitation of HME processing would mitigate moderate differences in the affinity of ITZ for the different polymer phases seen under the static heating conditions of DSC analysis to yield a homogenous composite.

### Analysis of Drug Distribution by EDS

To investigate the effect of Carbopol® 974P on the dispersed sate of ITZ in an EUDRAGIT® L 100-55-based matrix carrier system, EDS analysis was performed on the 40% Carbopol® 974P formulation as well as the HME processed ITZ/EUDRAGIT® L 100-55 (1:2) formulation for comparison. The EDS technique allows for elemental mapping of chlorine and nitrogen atoms over an STEM image which provides a visual representation of the distribution of these atoms in the imaged sample. In the analyzed formulations, chlorine and nitrogen atoms are present only on ITZ molecules, allowing this technique to be used to map the distribution of drug in the polymer matrix providing a qualitative assessment of the homogeneity of the composite.

The results of the EDS analysis are shown in Fig. 3. These images demonstrate that chlorine and nitrogen atoms are uniformly distributed at the resolution of these images (~1 µm) in both the EUDRAGIT® L 100-55-based sample as well as the EUDRAGIT® L 100-55/Carbopol® 974P (3:2)-based sample. The homogenous distribution of these elements in the polymer matrices indicates that ITZ is homogeneously distributed in both samples. Inferences, concerning the dispersion of ITZ in the different polymer phases of the 40% Carbopol® 974P formulation cannot be made by this technique; however, if ITZ exists primarily within the Carbopol® 974P phase, as the DSC results may suggest, the EDS images demonstrate that the Carbopol® 974P and EUDRAGIT® L 100-55 phases are well mixed.

### Dissolution Analysis with pH Change

To investigate the stabilizing effect of Carbopol® 974P on the supersaturation of ITZ in neutral pH media, the 20% and 40% Carbopol® 974P formulations were evaluated against the EUDRAGIT® L 100-55 carrier system by a pH switch dissolution method. The results of this dissolution analysis are presented in Fig. 4. The release of ITZ from the EUDRAGIT® L 100-55 matrix was minimal in acid (~4 mg), but rapid following the pH change with peak ITZ release (33 mg) occurring 10 min into the neutral phase of dissolution testing. Supersaturation of ITZ in neutral media was found to be transient with the EUDRAGIT® L 100-55 carrier system as ITZ concentration fell below quantifiable levels only 1 h after the pH change. The addition of 20% Carbopol® 974P to the EUDRAGIT® L 100-55 matrix reduced the acid phase release at 2 h (~2 mg) and retarded ITZ release following the pH transition with the maximum ITZ release (~15 mg) occurring 30 min after the pH change. However, the duration of supersaturation was substantially improved by the 20% Carbopol® 974P additive as 8 and 1.5 mg ITZ remain in solution 1 and 2 h after the pH change, respectively. Although these solution levels may appear slight, they represent 8,000 and 1,600-fold levels of ITZ supersaturation based on an estimated 1 ng/ml equilibrium solubility of ITZ at neutral pH (16).

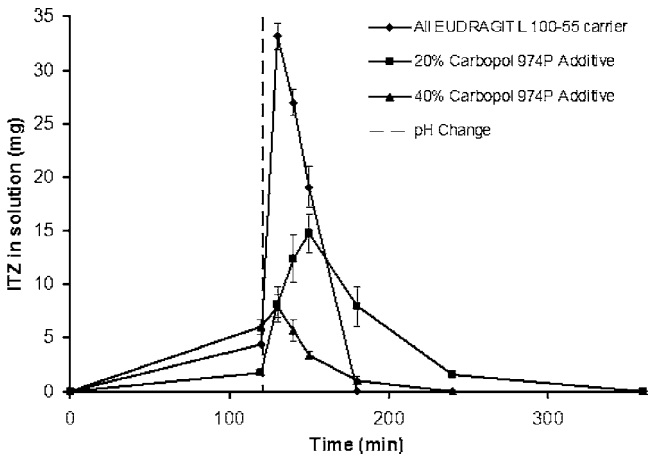


**Fig. 4.** Supersaturation dissolution testing of the 20% Carbopol® 974P additive formulation, the 40% Carbopol® 974P additive formulation, as well as an all EUDRAGT® L 100-55 carrier system by pH change method. Each dissolution vessel ($n$=4) contained 180 mg of the formulation (60 mg ITZ equivalent) corresponding to 20 times the saturation solubility of ITZ in the acid phase. Testing was conducted for 2 h in 750 ml of 0.1 N HCl followed by pH adjustment to 6.8±0.5 with 250 ml of 0.2 M tribasic sodium phosphate solution.

The inclusion of 40% Carbopol® 974P to the EUDRAGIT® L 100-55 carrier matrix generated a slight increase in the acid phase release at 2 h (6 mg), but substantially retarded release following the pH change with a peak ITZ release of only 8 mg occurring 10 min after the pH change. The duration of ITZ supersaturation with the 40% Carbopol® 974P formulation was improved over the EUDRAGIT® L 100-55 carrier system as ITZ concentrations of approximately 1,000 ng/ml were detected 1 h after the pH change. However, the duration of supersaturation achieved with the 40% Carbopol® 974P formulation was found to be inferior to the 20% Carbopol® 974P formulation as indicated by an eight-fold reduction in ITZ supersaturation 1 h after the pH change. Additionally, ITZ supersaturation was negligible 2 h after the pH change with the 40% Carbopol® 974P formulation, whereas supersaturated ITZ concentrations remained substantial 2 h after the pH change with the 20% Carbopol® 974P formulation.

Area under the dissolution curve (AUDC) values were calculated for the acidic phase ($AUDC_{acid}$), neutral phase ($AUDC_{neutral}$), and the total dissolution test ($AUDC_{total}$) for each evaluated composition to provide a quantitative means of comparing the extent of supersaturation produced by each formulation at each stage of dissolution testing. These results are provided in Table II. The AUDC results reveal that the greatest total extent of supersaturation was produced by the EUDRAGIT® L 100-55 formulation while the greatest acid phase release was produced by the 40% Carbopol® 974P formulation. However, the $AUDC_{neutral}$ value is the key metric by which to evaluate the different compositions as it is expected to correlate directly to *in vivo* absorption. The EUDRAGIT® L 100-55 and the 20% Carbopol® 974P formulations showed essentially equivalent $AUDC_{neutral}$ values of 1,005 and 1,006 mg·min respectively, while the 40% Carbopol® 974P formulation produced a substantially lower $AUDC_{neutral}$ value of 284 mg·min.

The transient nature of ITZ release from the EUDRAGIT® L 100-55 formulation following the pH change was hypothesized to be the underlying cause of the *in vivo* absorption variability observed with this formulation from our previous report (2). Eliminating the pulsed nature of ITZ release from this formulation by the incorporation of a stabilizing additive that extends ITZ supersaturation along the proximal small intestine is expected to reduce variability and while improving absorption. The results of this dissolution study demonstrate both the retardant and stabilizing effects of Carbopol® 974P on the release of ITZ from an EUDRAGIT® L 100-55 matrix in neutral pH media.

The retardant effects of Carbopol® polymers on drug release from solid dosage forms has been well documented in the pharmaceutical literature (25–29). Carbopol® polymers swell in neutral media owing to the ionization of carboxylic acid groups resulting in the formation of a viscous hydrogel that retards drug diffusion from the swollen polymer matrix. This effect is clearly seen in Fig. 4 as the rate of ITZ release from the EUDRAGIT® L 100-55 matrix following the pH change was substantially reduced in accordance with the concentration of Carbopol® 974P in the formulation. Following the pH transition, ITZ which has been hydrated in the acid phase is immediately released from the EUDRAGIT® L 100-55 matrix upon polymer dissolution. When Carbopol® 974P is added to the formulation, the viscosity in the vicinity of dissolved ITZ is substantially increased in proportion to the amount of Carbopol® 974P in the formulation. Therefore, ITZ pre-hydrated by the acidic medium is not immediately released into solution following the pH change where it is unstable and rapidly precipitates, but rather the release of ITZ is controlled and prolonged by the viscous Carbopol® 974P gel. This controlled release effect is expected to prolong the presence of supersaturated ITZ in the small intestine thereby providing a greater opportunity for ITZ absorption.

The retardant effect of Carbopol® 974P is therefore advantageous with regards to transforming the pulsed, transient ITZ release profile from the EUDRAGIT® L 100-55 matrix into a more sustained supersaturated release profile. Carbopol® 974P at 20% of the polymer carrier proved to be the ideal concentration as the $AUDC_{neutral}$ value remained equivalent to that of the EUDRAGIT® L 100-55 formulation; however, the release profile was substantially more prolonged. The addition of Carbopol® 974P at 40% of the polymer weight proved to be excessively retardant as the $AUDC_{neutral}$ value was reduced by a factor of 3.5. Based on this result, it is expected that this formulation would produce substantially lower absorption than the formulation containing only 20% Carbopol® 974P additive.

The extended release profile of ITZ from the EUDRAGIT® L 100-55/Carbopol® 974P matrix would not be possible if the polymers did not provide adequate stabilization of ITZ solubilized within the swollen Carbopol® 974P matrix. Carbopol® 974P contains an abundance of acidic functional groups on the polymer chains and the viscosity of the polymer network swollen in neutral pH media is substantial. This combination provides the ideal microenvironment for stabilizing ITZ in neutral solution. Numerous hydrogen bond donor sites are available to interact with and stabilize ITZ molecules in solution while the high viscosity of the gel retards ITZ diffusion and thus maintains these stabilizing interactions for greater durations.

This proposed interaction of ITZ with the acidic functional groups on the carrier polymers is in agreement with the drug-polymer salt formation mechanism proposed by van den Mooter *et al.* (23) and the maintenance of this electrostatic interaction in solution is apparently prolonged by increasing the viscosity of the acidic polymer. In terms of

**Table II.** Area Under the Dissolution Curve (AUDC) Values for the Acid Phase, Neutral Phase and Total Dissolution Test for the EUDRAGIT® L 100-55, 20% Carbopol® 974P, and 40% Carbopol® 974P Formulations

| Polymer Carrier | $AUDC_{acid}$ (mg·min) | $AUDC_{neutral}$ (mg·min) | $AUDC_{total}$ (mg·min) |
|---|---|---|---|
| EUDRAGIT® L 100-55 | 263±6 | 1,005±60 | 1,268±62 |
| 20% Carbopol® 974P | 103±9 | 1,006±156 | 1,110±148 |
| 40% Carbopol® 974P | 362±42 | 284±39 | 645±65 |

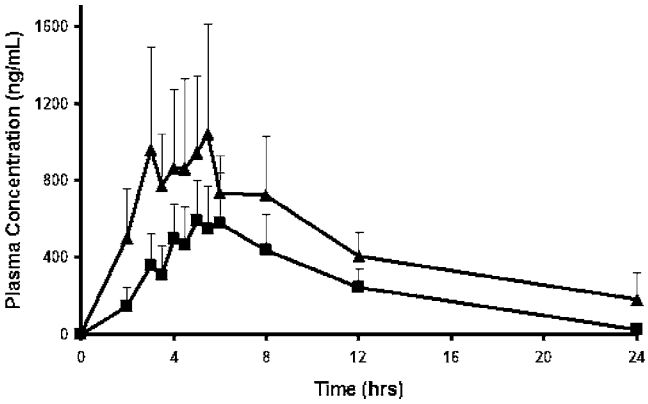


**Fig. 5.** Plasma ITZ concentration *versus* time from oral dosing of (*filled triangle*) 20% Carbopol® 974P additive formulation and (*filled square*) 40% Carbopol® 974P additive formulation. The doses were administered by oral gavage in the amount of 30 mg ITZ/kg body weight per subject in rats ($n$=4).

crystallization kinetics, when the drug is in strong association with the polymer and polymer viscosity retards diffusion of drug molecules into bulk solution, this will decrease the rate of nuclei formation and subsequent particle growth. Ultimately the result is delayed precipitation, and thus prolongation of supersaturation.

The results of this dissolution study revealed that owing to its retardant and stabilizing properties, the addition of 20% Carbopol® 974P to the EUDRAGIT® L 100-55 carrier system provided a prolonged ITZ release profile following the acid to neutral pH change without limiting the $AUDC_{neutral}$ value. It is expected that this formulation will produce greater absorption with less variability than the EUDRAGIT® L 100-55 carrier system alone by extending the duration for which the intestinal mucosa is exposed to supersaturated levels of ITZ.

### *In vivo* ITZ Absorption Analysis

To examine the effect of the Carbopol® 974P additive on the *in vivo* absorption of ITZ, oral dosing studies were conducted with both the 20% and 40% Carbopol® 974P formulations in male Sprague–Dawley rats. The plasma concentration *versus* time profiles are presented in Fig. 5 and the pharmacokinetic data are presented in Table III. Qualitatively, greater absorption was achieved with the 20% Carbopol® 974P formulation than with the 40% Carbopol® 974P formulation, although both formulations produced substantial ITZ absorption. The plasma concentration profile with the 20% Carbopol® 974P formulation shows two peak ITZ plasma concentrations appearing at 3 and 5.5 h. This dual-peak shape was also reported in our previous report (2) for both the Methocel™ E50 and EUDRAGIT® L 100-55 formulations and was attributed to enterohepatic recirculation of unmetabolized ITZ as was reported to occur with high ITZ doses by Hardin *et al.* (30).

The pharmacokinetic data confirms that the overall absorption generated by the 20% Carbopol® 974P formulation was greater than that of the 40% Carbopol® 974P formulation with respective mean AUC values of 11,107 and 5,830 ng·h/ml. These mean AUC values were determined to be statistically different ($p$=0.04 (two tailed)). Although not statistically significant, the mean $C_{max}$ value was also greater with the 20% than the 40% Carbopol® 974P formulation with respective values of 1,198 and 662 ng/ml. The $T_{max}$ values between the 20% and 40% Carbopol® 974P formulations were roughly equivalent (4.4±1.6 and 5.6±0.5 h, respectively), but the mean $T_{1/2}$ was greater with the 20% than the 40% Carbopol® 974P additive although the difference was not statistically significant (7.9±3.7 and 4.7±1.9 h, respectively).

These *in vivo* results demonstrate that the addition of Carbopol® 974P substantially reduces the variability of ITZ absorption from the EUDRAGIT® L 100-55 carrier system. The absorption variability with the EUDRAGIT® L 100-55 formulation from our previous paper (2) was found to be 140%. The addition of 20% and 40% Carbopol® 974P to the EUDRAGIT® L 100-55 matrix reduced this absorption variability to 32% and 33%, respectively. *In vitro*, both Carbopol® 974P additive formulations demonstrated improved duration of supersaturation over the EUDRAGIT® L 100-55 carrier system. The transient ITZ supersaturation profile of the EUDRAGIT® L 100-55 carrier system was markedly transformed to a more prolonged ITZ supersaturation profile by the Carbopol® 974P additives. The prolongation of intestinal membrane exposure to supersaturated ITZ caused by this alteration in release profile is the most likely cause for the improvement in absorption variability.

*In vitro*, the 20% Carbopol® 974P formulation exhibited substantially improved extent and duration of ITZ supersaturation over the 40% Carbopol® 974P formulation as indicated by the 3.5-fold increase in $AUDC_{neutral}$ value. In relation to *in vivo* absorption, this *in vitro* result indicates that the 20% Carbopol® 974P formulation would expose the intestinal mucosa to greater ITZ concentrations for an extended duration than the 40% Carbopol® 974P formulation. Therefore, it is not surprising that an almost two-fold improvement in ITZ absorption was generated by the 20% Carbopol® 974P formulation over the 40% Carbopol® 974P formulation.

Compared to the ITZ/Methocel™ E50 (1:2) formulation, identified as the best composition with regard to *in vivo* absorption from our previous report (2), the 20% Carbopol® 974P formulation exhibited a near two-fold improvement in AUC. The mean AUC values of the Methocel™ E50 and 20% Carbopol® 974P were determined to be statistically different ($p$=0.04 (two tailed)). Compared to our previous report regarding the immediate release particulate dispersion

**Table III.** Pharmacokinetic Data from the *In vivo* Absorption Study with the 20% Carbopol® 974P Additive Formulation and the 40% Carbopol® 974P Additive Formulation ($n$=4 per group)

| Formulation | $C_{max}$ (ng/ml) | $T_{max}$ (h) | AUC (ng·h/ml) | $T_{1/2}$ (h) |
|---|---|---|---|---|
| 20% Carbopol Additive | 1,198±584 | 4.4±1.6 | 11,107±3,579 | 7.94±3.7 |
| 40% Carbopol Additive | 663±186 | 5.6±0.5 | 5,830±1,943 | 4.7±1.9 |
| $p$ value (two tail) | 0.13 | 0.19 | 0.04 | 0.18 |

compositions (negligible supersaturation at neutral pH) (1), the 20% Carbopol® 974P formulation generated a five-fold increase in total ITZ absorption. A similar five-fold improvement in ITZ absorption was also achieved with the 20% Carbopol® 974P formulation as compared to Sporanox® capsules which were evaluated for ITZ absorption in a similar *in vivo* study conducted by Lee *et al.* in male Sprague–Dawley rats (31). The dose was 33% lower in the study by Lee *et al.* than in the current study; however, on a dose normalized basis a 3.4-fold improvement in AUC was achieved with the 20% Carbopol® 974P formulation over the Sporanox® capsule formulation. This improvement therefore suggests the superiority of the 20% Carbopol® 974P additive formulation over the current solid oral ITZ commercial product.

Interestingly, the 40% Carbopol® 974P formulation showed statistically equivalent absorption to the Methocel™ E50 formulation presented in our previous paper (2) despite a seven-fold lower $AUDC_{neutral}$ value. This result is most likely attributable to the viscous gel formation of Carbopol® 974P in neutral pH media which stabilizes ITZ in neutral pH media via strong intermolecular interactions that are supplemented by high local viscosity. Therefore, ITZ is thermodynamically more stable in the Carbopol® 974P gel than in bulk, neutral pH solution. Hence, there exists an enthalpic barrier, in addition to the viscous physical barrier, that holds ITZ molecules in the gel network and limits diffusion into bulk solution. *In vitro*, this effect gives rise to poor ITZ release. *In vivo*, when the ITZ loaded Carbopol® 974P gel makes contact with the intestinal mucosa, the enthalpic barrier retaining ITZ inside the gel is reduced and ITZ will preferentially partition into the hydrophobic intestinal membrane. This gel-to-membrane partitioning effect may explain the discrepancy between the $AUDC_{neutral}$ *in vitro* metric and the *in vivo* absorption seen with the 40% Carbopol® 974P formulation. Similar gel-to-membrane partitioning effects with lipophilic drugs have been reported in the pharmaceutical literature (32–34).

With only 20% Carbopol® 974P in the formulation, more ITZ is released into bulk solution with this formulation than with the 40% Carbopol® 974P formulation as a result of reduced gel formation/local viscosity. Consequently, a large portion of absorption occurs by supersaturation of the intestinal lumen with ITZ and the gel-to-membrane partitioning of ITZ serves as an additional mechanism of absorption. When comparing the *in vitro* and *in vivo* performance of the 20% Carbopol® 974P formulation *versus* the Methocel™ E50 formulation, the supplementary effect of the gel-to-membrane ITZ permeation becomes apparent as the 20% Carbopol® 974P formulation produced a near two-fold lower $AUDC_{neutral}$ value than the Methocel™ E50 formulation, yet generated nearly twice the *in vivo* absorption. This comparison suggests that the supersaturation of intestinal lumen provided by the dissolution of EUDRAGIT® L 100-55 coupled with the hydrogel forming effects of Carbopol® 974P act synergistically to vastly improve ITZ absorption in the small intestine.

Based on reports in the pharmaceutical literature describing the mucoadhesive properties of Carbopol® polymers (35–40), it could be concluded that the *in vivo* absorption improvement provided by the formulations evaluated in this study are the result of mucoadhesion in the small intestine. However, the efficacy of mucoadhesion with Carbopol® polymers in the small intestine has not been adequately proven (41–44), and therefore to attribute the absorption enhancement entirely to the mucoadhesive properties of Carbopol® would not be justified. The strong affinity of Carbopol® 974P for the intestinal mucosa likely increases the intimacy of contact between supersaturated ITZ contained within the gel and the intestinal membrane; however, the principal cause of absorption enhancement can likely be attributed to the highly viscous character of the Carbopol® 974P gel in the neutral pH environment which resulted in prolonged intestinal transit time. Increased transit time in the upper small intestine coupled with more intimate contact of dissolved ITZ with the intestinal mucosa would promote the gel-to-membrane partitioning of ITZ and could explain the substantial discrepancy between the $AUDC_{neutral}$ values and the *in vivo* absorption for both Carbopol® 974P additive formulations.

## CONCLUSIONS

This study demonstrated the stabilizing effect of Carbopol 974P on supersaturated levels of ITZ *in vitro* and its absorption enhancing effects *in vivo* when incorporated into an EUDRAGIT® L 100-55 carrier matrix. The combination of these polymers as a carrier for amorphous ITZ yields a targeted intestinal delivery system which is able to generate prolonged supersaturation of ITZ within the small intestine. The considerable increase in AUC achieved with the 20% Carbopol® 974P formulation over our previously reported compositions, as well as results reported in the literature for Sporanox® capsules, demonstrates a tremendous improvement in the oral absorption of ITZ. These results strongly suggest the potential for improved antifungal therapy with orally delivered ITZ via intestinal targeting with prolonged supersaturation. Furthermore, it is believed that this delivery system could be broadly applied to other poorly water-soluble drugs with pH-dependant solubility profiles similar to ITZ to improve absorption and ultimately increase the bioavailability of these therapeutic compounds.

## ACKNOWLEDGEMENTS

The authors would like to thank Dr. J. P. Zhou for his assistance with TEM Imaging.

## REFERENCES

1. D. A. Miller, J. T. McConville, W. Yang, R. O. Williams III, and J. W. McGinity. Hot-melt extrusion for enhanced delivery of drug particles. *J. Pharm. Sci* **96**(2):361–376 (2007).
2. D. A. Miller, J. C. DiNunzio, W. Yang, J. W. McGinity, and R. O. Williams III. Enhanced *In vivo* Absorption of Itraconazole via Stabilization of Supersaturation Following Acidic-to-Neutral pH Transition Drug Development and Industrial Pharmacy 2007;(in press) DOI 10.1080/03639040801929273.
3. W. S. Snyder, M. J. Cook, E. S. Nasset, L. R. Karhausen, G. P. Howells, and I. H. Tipton. *Report of the Task Group on Reference Man*. Pergamon Press, New York, 1975.
4. J. M. DeSesso, and C. F. Jacobson. Anatomical and physiological parameters affecting gastrointestinal absorption in humans and rats. *Food Chem. Toxicol* **39**(3):209–228 (2001).
5. M. Mayersohn. Principles of Drug Absorption. In G. S. Banker, and C. T. Rhodes (eds.), *Modern Pharmaceutics*, Marcel Dekker, New York, 1996, pp. 21–74.

6. D. A. Miller, J. W. McGinity, and R. O. Williams III. Solid dispersion technologies. In R. O. Williams III, D. R. Taft, and J. T. McConville (eds.), *Advanced Drug Formulation Design to Optimize Therapeutic Outcomes*, Informa Healthcare USA, New York, NY, USA, 2007, pp. 451–491.
7. P. Gao, M. E. Guyton, T. Huang, J. M. Bauer, K. J. Stefanski, and Q. Lu. Enhanced oral bioavailability of a poorly water soluble drug PNU-91325 by supersaturatable formulations. *Drug Dev. Ind. Pharm* **30**(2):221–229 (2004).
8. P. Gao, and W. Morozowich. Development of supersaturatable self-emulsifying drug delivery system formulations for improving the oral absorption of poorly soluble drugs. *Expert Opinion on Drug Delivery* **3**(1):97–110 (2006).
9. R. Vandecruys, J. Peeters, G. Verreck, and M. E. Brewster. Use of a screening method to determine excipients which optimize the extent and stability of supersaturated drug solutions and application of this system to solid formulation design. *Int. J. Pharm* **342**(1–2):168–175 (2007).
10. M. E. Brewster, and T. Loftsson. Cyclodextrins as pharmaceutical solubilizers. *Adv. Drug Deliv. Rev* **59**(7):645–666 (2007).
11. N. Kondo, T. Iwao, K. Hirai, M. Fukuda, K. Yamanouchi, K. Yokoyama, M. Miyaji, Y. Ishihara, and K. Kon. Improved Oral Absorption of Enteric Coprecipitates of a Poorly Soluble Drug. *J. Pharm. Sci* **83**(4):566–570 (1994).
12. N. Kohri, Y. Yamayoshi, H. Xin, K. Iseki, N. Sato, S. Todo, and K. Miyazaki. Improving the oral bioavailability of albendazole in rabbits by the solid dispersion technique. *J. Pharm. Pharmacol* **51**(2):159–164 (1999).
13. N. Kohri, Y. Yamayoshi, K. Iseki, N. Sato, S. Todo, and K. Miyazaki. Effect of gastric pH on the bioavailability of albendazole. *Pharm. Pharmacol. Commun* **4**:267–270 (1998).
14. Carbopol® 974P NF Polymer—Product Specification. 2007 (accessed August 2007, at www.lubrizol.com.).
15. D. A. Miller, M. Gamba, D. Sauer, T. P. Purvis, N. T. Clemens, and R. O. Williams III. Evaluation of the USP dissolution test method A for enteric-coated articles by planar laser-induced fluorescence. *Int. J. Pharm* **330**(1–2):61–72 (2007).
16. J. Peeters, P. Neeskens, J. P. Tollenaere, P. Van Remoortere, and M. Brewster. Characterization of the interaction of 2-hydroxypropyl-B-cyclodextrin with itraconazole at pH 2, 4 and 7. *J. Pharm. Sci* **91**:1414–1422 (2002).
17. P. O. Gubbins, B. J. Gurley, and J. Bowman. Rapid and sensitive high performance liquid chromatographic method for the determination of itraconazole and its hydroxy-metabolite in human serum. *J. Pharm. Biomed. Anal* **16**:1005–1012 (1998).
18. J. M. Vaughn, J. T. McConville, D. Burgess, J. I. Peters, K. P. Johnston, R. L. Talbert, and R. O. Williams Iii. Single dose and multiple dose studies of itraconazole nanoparticles. *Eur. J. Pharm. Biopharm* **63**(2):95–102 (2006).
19. K. A. Overhoff, A. Moreno, D. A. Miller, K. P. Johnston, and R. O. Williams Iii. Solid dispersions of itraconazole and enteric polymers made by ultra-rapid freezing. *Int. J. Pharm* **336**(1):122–132 (2007).
20. K. Six, C. Leuner, J. Dressman, G. Verreck, J. Peeters, N. Blaton, P. Augustijns, R. Kinget, and G. Van den Mooter. Thermal Properties of Hot-Stage Extrudates of Itraconazole and Eudragit E100. Phase separation and polymorphism. *J. Therm. Anal. Calorim* **68**(2):591–601 (2002).
21. K. Six, J. Murphy, I. Weuts, D. Q. M. Craig, G. Verreck, J. Peeters, M. Brewster, and G. Van den Mooter. Identification of Phase Separation in Solid Dispersions of Itraconazole and Eudragit® E100 Using Microthermal Analysis. *Pharm. Res* **20**(1):135–138 (2003).
22. K. Six, G. Verreck, J. Peeters, M. E. Brewster, and G. Van den Mooter. Increased physical stability and improved dissolution properties of itraconazole, a class II drug, by solid dispersions that combine fast- and slow-dissolving polymers. *J. Pharm. Sci* **93**(1):124–131 (2004).
23. G. van den Mooter, G. Verreck, M. Brewster, J. Peeters, I. Weuts, A. DeCorte, K. Heymans, D. Kempen. inventors; Janssen Pharmaceutica N.V., assignee. Solid Dispersions of a Basic Drug Compound and a Polymer Containing Acidic Groups patent WO/2005/117834. 2005.
24. K. Six, G. Verreck, J. Peeters, K. Binnemans, H. Berghmans, P. Augustijns, R. Kinget, and G. Van den Mooter. Investigation of thermal properties of glassy itraconazole: identification of a monotropic mesophase. *Thermochimica Acta* **376**(2):175–181 (2001).
25. L. Huang, and J. Schwartz. Studies on drug release from a carbomer tablet matrix. *Drug Dev. Ind. Pharm* **21**(13):1487–501 (1995).
26. V. R. Goskonda, I. K. Reddy, M. J. Durrani, W. Wilber, and M. A. Khan. Solid-state stability assessment of controlled release tablets containing Carbopol(R) 971P. *J. Control. Release* **54**(1):87–93 (1998).
27. M. M. Meshali, G. M. El-Sayed, Y. El-Said, and H. M. El-Aleem. Preparation and evaluation of theophylline sustained release tablets. *Drug Dev. Ind. Pharm* **22**:373–376 (1996).
28. B. Perez-Marcos, J. L. Ford, D. J. Armstrong, P. N. Elliott, and J. E. Hogan. Release of propranolol hydrochloride from matrix tablets containing hydroxypropyl methyl cellulose K4M and Carbopol 974. *Int. J. Pharm* **111**:251–259 (1994).
29. S. Neau, M. Chow, and M. J. Durrani. Fabrication and characterization of extruded and spheronized beads containing Carbopol 974P NF resin. *Int. J. Pharm* **131**:47–55 (1996).
30. T. C. Hardin, J. R. Graybill, R. Fetchick, R. Woestenborghs, M. G. Rinaldi, and J. G. Kuhn. Pharmacokinetics of itraconazole following oral administration to normal volunteers. *Antimicrob. Agents Chemother.* **32**(9):1310–1313 (1988).
31. S. Lee, K. Nam, M. S. Kim, S. W. Jun, J. S. Park, J. S. Woo, and S. J. Hwang. Preparation and characterization of solid dispersions of itraconazole by using aerosol solvent extraction system for improvement in drug solubility and bioavailability. *Arch. Pharm. Res.* **28**(7):866–874 (2005).
32. A. J. Ribeiro, R. J. Neufeld, P. Arnaud, and J. C. Chaumeil. Microencapsulation of lipophilic drugs in chitosan-coated alginate microspheres. *Int. J. Pharm* **187**(1):115–123 (1999).
33. A. Fahr, P. V. Hoogevest, S. May, N. Bergstrand, and M. L. S. Leigh. Transfer of lipophilic drugs between liposomal membranes and biological interfaces: Consequences for drug delivery. *Eur. J. Pharm. Sci* **26**(3–4):251–265 (2005).
34. K. Moser, K. Kriwet, C. Froehlich, Y. N. Kalia, and R. H. Guy. Supersaturation: Enhancement of Skin Penetration and Permeation of a Lipophilic Drug. *Pharm. Res* **18**:1006–1011 (2001).
35. H. Takeuchi, H. Yamamoto, and Y. Kawashima. Mucoadhesive nanoparticulate systems for peptide drug delivery. *Adv. Drug Deliv. Rev.* **47**(1):39–54 (2001).
36. A. Singla, M. Chawla, and A. Singh. Potential applications of carbomer in oral mucoadhesive controlled drug delivery system: a review. *Drug Dev. Ind. Pharm.* **26**:913–924 (2000).
37. J. Llabot, R. Manzo, and D. Allemandi. Drug release from carbomer:carbomer sodium salt matrices with potential use as mucoadhesive drug delivery system. *Int. J. Pharm* **276**:59–66 (2004).
38. K. P. R. Chowdary, and Y. S. Rao. Design and *In vitro* and *In vivo* Evaluation of Mucoadhesive Microcap-sules of Glipizide for Oral Controlled Release: A Technical Note. *AAPS PharmSciTech* **4**(3):1–6 (2003).
39. G. Borchard, H. L. Lueen, A. G. de Boer, J. C. Verhoef, C.-M. Lehr, and H. E. Junginger. The potential of mucoadhesive polymers in enhancing intestinal peptide drug absorption. III: Effects of chitosan-glutamate and carbomer on epithelial tight junctions *in vitro*. *J. Control. Release* **39**(2–3):131–138 (1996).
40. A. Bernkop-Schnurch, B. Gilge. Anionic Mucoadhesive Polymers as Auxiliary Agents for the Peroral Administration of (Poly)Peptide Drugs: Influence of the Gastric Juice. In: Informa Healthcare, 2000, pp. 107–113.
41. N. Thirawong, J. Nunthanid, S. Puttipipatkhachorn, and P. Sriamornsak. Mucoadhesive properties of various pectins on gastrointestinal mucosa: An *in vitro* evaluation using texture analyzer. *Eur. J. Pharm. Biopharm* **67**(1):132–140 (2007).
42. S. S. Davis. Formulation strategies for absorption windows. *Drug Discov. Today* **10**(4):249–257 (2005).
43. A. Bernkop-Schnurch, and A. Greimel. Thiomers: The next generation of mucoadhesive polymers. *American Journal of Drug Delivery* **3**(3):141–154 (2005).
44. N. A. Peppas, and Y. Huang. Nanoscale technology of mucoadhesive interactions. *Adv. Drug Deliv. Rev* **56**(11):1675–1687 (2004).